Matrix-Isolation Fourier Transform Infrared and Theoretical Studies of Laser-Ablated Sc Atom Reactions with Water Molecules

Luning Zhang, Jian Dong, and Mingfei Zhou*

Laser Chemistry Institute, Fudan University, Shanghai 200433, P.R.China

Received: May 17, 2000; In Final Form: July 17, 2000

Laser-ablated Sc atoms have been reacted with water molecules during condensation with argon at 11 K. In agreement with previous thermal atom reactions, absorptions at 1482.6 and 713.0 cm^{-1} are assigned to the HScOH molecule formed via an insertion reaction. Photolysis of the HScOH produces the metal monoxide ScO. In addition, new absorption at 765.6 cm^{-1} is also observed and is assigned to the ScOH molecule. The ScOH molecule undergoes photoinduced rearrangement to the HScO molecule, which is characterized by Sc−H and Sc−O stretching vibrations at 1391.1 and 922.3 cm^{-1}. Density functional theoretical calculations have been performed for the aforementioned species, and important transition states on the reaction paths have been obtained.

Introduction

The interaction of metal atoms and cations with water molecules has attracted considerable experimental[1−9] and theoretical attention.[10−14] The reactions of transition metal cations and water have been studied in the gas phase and the formation of $MO^+ + H_2$ was found to be exothermic for early transition metal cations, while for middle transition metal cations, no exothermic products were observed.[1−3] Several theoretical works have also been carried out concerning the reactivity of transition metal cations with water molecules, which provided new insights into likely reaction intermediates, various possible transition states, and products.[10−14]

Lin and Parson reported that atomic Sc reacted with water to give ScO in the gas phase.[5] Matrix isolation infrared absorption studies showed that thermal Sc atoms reacted with water to form the insertion products spontaneously, while the metal monoxides were formed on photolysis.[7] To our knowledge, there is no theoretical study on Sc atom reactions with water, and the reaction pathway concerning metal atom reactions with water are not clear.

It is well-known that laser ablation of the metal target can produce ground-state metal atoms as well as excited-state atoms with high kinetic energy. Recent investigations of laser-ablated transition metal atom reactions with small molecules have shown very rich chemistry due to higher reactivity of the ablated metal species, and more products were observed as compared with thermal atom reactions.[15−17] In this paper, we present a combined matrix-isolation FTIR and theoretical investigation on the reactions of laser-ablated Sc atoms with water molecules.

Experimental and Theoretical Methods

The experimental setup for pulsed laser ablation and matrix infrared spectroscopic investigation has been described previously[18] and is very similar to the technique employed earlier by the Andrews group.[19] The 1064 nm Nd:YAG laser fundamental (Spectra Physics, DCR 150, 20 Hz repetition rate and 8 ns pulse width) was focused onto the rotating Sc target through a hole in a CsI window, and the ablated metal atoms were codeposited with H_2O in excess argon onto a 11 K CsI window, which was mounted on a cold tip of a closed-cycle helium refrigerator (Air Products, model CSW202) for 1 h at a rate of 4−5 mmol/h. Typically, a 5−10 mJ/pulse laser power was used and focused into a spot of about 0.25 mm^2 on the target. At this controlled laser fluence, we managed to generate a plume containing enough hot metal atoms and electrons for reaction and also prevent excessive high-energy UV photons to deplete the products. H_2O, $H_2{}^{18}O$(96%^{18}O), and D_2O were subjected to several freeze−pump−thaw cycles before use. Infrared spectra were recorded on a Bruker IFS113v spectrometer at 0.5 cm^{-1} resolution using a DTGS detector. Matrix samples were annealed at different temperatures, and selected samples were subjected to broadband photolysis using a high-pressure mercury lamp.

Quantum chemical calculations were performed using the Gaussian 98 program.[20] The three-parameter hybrid functional according to Becke with additional correlation corrections due to Lee, Yang, and Parr were utilized (B3LYP).[21,22] Recent calculations have shown that this hybrid functional can provide accurate results for the geometries and vibrational frequencies for transition metal containing compounds.[12−14,23,24] The 6-311++G(d,p) basis sets were used for H and O atoms, and the all electron basis sets of Wachters-Hay as modified by Gaussian were used for the Sc atom.[25,26] Reactants, various possible transition states, intermediates, and products were optimized. The vibrational frequencies were calculated with analytic second derivatives, and zero point vibrational energies (ZPVE) were derived.

Results and Discussion

Infrared Spectra. Infrared spectra for the reaction of laser-ablated Sc atoms with water molecules in excess argon in the 1520−1380, 980−900, and 780−680 cm^{-1} regions are illustrated in Figure 1, and the absorptions are listed in Table 1. The stepwise annealing and photolysis behavior of these product absorptions are also shown and will be discussed below. D_2O and $H_2{}^{18}O$ samples were employed for product identification through isotopic shift and splitting, the isotopic counterparts

* Corresponding author. E-mail: mfzhou@srcap.stc.sh.cn.

10.1021/jp001836r CCC: $19.00
Published on Web 09/08/2000

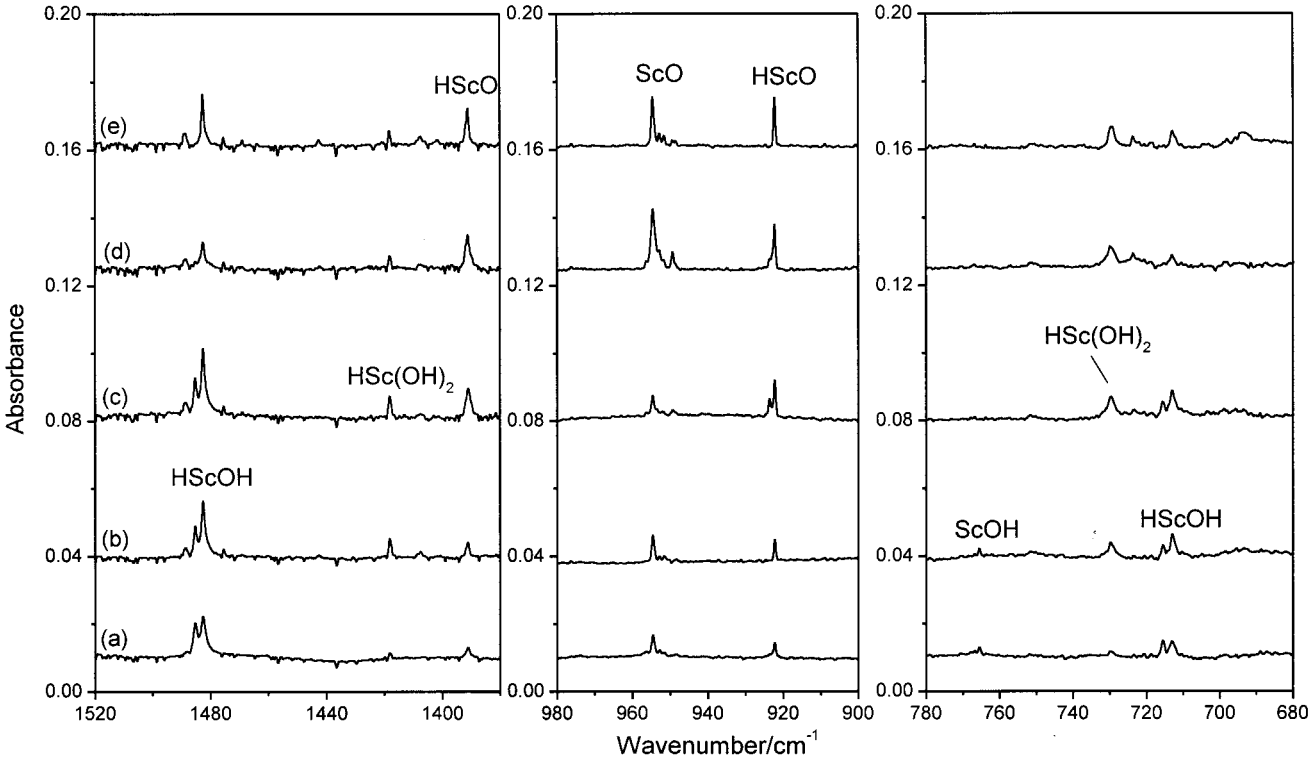

Figure 1. Infrared spectra in the 1520−1380, 980−900, and 780−680 cm^{-1} regions from codeposition of laser-ablated Sc atoms with 0.5% H_2O in argon: (a) 1 h sample deposition at 11 K; (b) after 25 K annealing; (c) after 20 min $\lambda > 400$ nm photolysis; (d) after 20 min $\lambda > 250$ nm photolysis; (e) after 30 K annealing.

TABLE 1: Infrared Absorptions (cm^{-1}) from Codeposition of Laser-Ablated Sc Atoms and Water Molecules in Excess Argon at 11 K

H_2O	$H_2{}^{18}O$	D_2O	assignment
1485.3	1485.2		HScOH site
1482.6	1482.6	1068.5	HScOH (Sc−H str)
1418.3			$HSc(OH)_2$ (Sc−H str)
1391.1	1390.8	1004.2	HScO (Sc−H str)
954.7	915.0	954.7	ScO
922.3	884.3	922.3	HScO (Sc−O str)
765.6	736.9	750.5	ScOH (Sc−OH str)
729.6	709.5	713.3	$HSc(OH)_2$ (Sc−$(OH)_2$ asy str)
715.7	692.1	696.9	HScOH site
713.0	689.1	693.6	HScOH (HSc−OH str)

are also listed in Table 1. The spectra with mixed $H_2O + D_2O$ in the 1100−980 and 780−680 cm^{-1} regions are shown in Figure 2. Figure 3 shows the spectra in the 1000−850 cm^{-1} region using a $H_2O + H_2{}^{18}O$ sample.

Calculation Results. B3LYP calculations were first done on scandium monoxide and hydride, and the results are listed in Table 2. The ScO was predicted to have a $^2\Sigma^+$ ground state with a bond length of 1.659 Å. Two states of the ScH molecule were calculated to be very close in energy, a $^3\Delta$ triplet state is about 1.7 kcal/mol lower in energy than a $^1\Sigma^+$ state. Previous experiments and calculations reported the $^1\Sigma^+$ to be the ground state,[27,28] our B3LYP/6-311++G(d,p) calculations predicted the relative stability of these two states in error.

Calculations were done on two [Sc,O,H] isomers, namely, HScO and ScOH. The calculated geometric parameters are shown in Figure 4, and the vibrational frequencies and intensities are listed in Table 3. The HScO has a $^1A'$ ground state with bent geometry ($\angle$HScO = 119.2°), with Sc−H and Sc−O bond lengths of 1.879 and 1.671 Å. The ScOH molecule was predicted to have a $^1\Sigma^+$ ground state with a $^3\Delta$ state lying only about 0.7 kcal/mol higher in energy. At the B3LYP/6-311++G(d,p) level

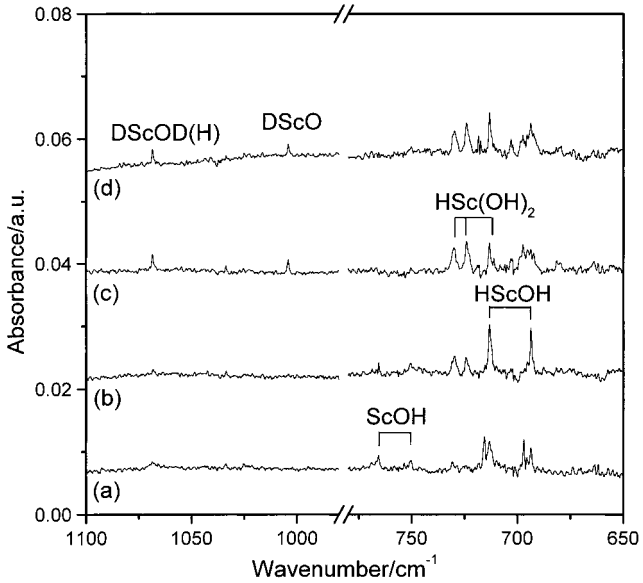

Figure 2. Infrared spectra in the 1100−980 and 780−680 cm^{-1} regions from codeposition of laser-ablated Sc atoms with 0.1% H_2O + 0.2% HDO + 0.1%D_2O in argon: (a) 1 h sample deposition at 11 K; (b) after 25 K annealing; (c) after 20 min $\lambda > 250$ nm photolysis; (d) after 30 K annealing.

of theory, the $^1A'$ HScO is about 6.8 kcal/mol more stable than the $^1\Sigma^+$ ScOH molecule.

Calculations were also done for two isomers of ScH_2O on the doublet potential energy surface, namely, the inserted HScOH molecule with C_s symmetry and the $ScOH_2$ complex with C_{2v} symmetry. For HScOH and $ScOH_2$, the values of S^2 are 0.752 and 0.778, respectively, suggesting negligible mild spin contamination. The geometric parameters of HScOH and $ScOH_2$ are shown in Figure 4, and the vibrational frequencies with IR intensities are listed in Table 4. The inserted HScOH

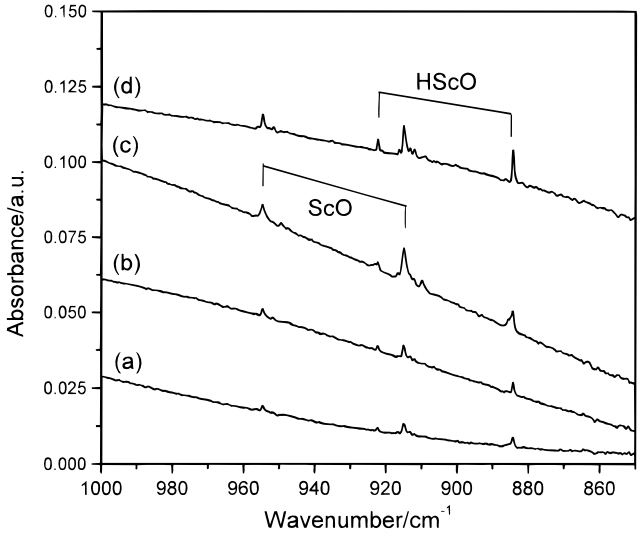

Figure 3. Infrared spectra in the 1000−850 cm^{-1} region from codeposition of laser-ablated Sc atoms with 0.1% H_2O + 0.4% $H_2{}^{18}O$ in argon: (a) 1 h sample deposition at 11 K; (b) after 25 K annealing; (c) after 20 min $\lambda > 250$ nm photolysis; (d) after 30 K annealing.

TABLE 2: Calculated Bond Length and Vibrational Frequencies of ScH and ScO

	bond length (Å)	frequency (intensity)
$ScH(^3\Delta)$	1.849	1483.8 (295)
$ScH(^1\Sigma^+)$	1.751	1626.3 (275)
$ScO(^2\Sigma^+)$	1.659	999.5 (211)
$H_2(^1\Sigma_g^+)$	0.744	4423.3 (0)
$H_2O(^1A_1)^a$	0.962	3922.2 (57), 3817.0 (9), 1602.5 (67)

[a] Bond angle: 105.1°.

molecule was predicted to have a $^2A'$ ground state with cis configuration. The $ScOH_2$ complex was predicted to have a $^2A_1$ ground state, which is about 48.0 kcal/mol higher in energy than the $^2A'$ HScOH molecule. As can be seen in Table 4, there is one imaginary frequency for the $^2A_1$ $ScOH_2$ molecule, suggesting that it is a first-order saddle point. Geometry optimization on H_2ScO converged to ScO + H_2.

Finally, similar calculation was also done on the $HSc(OH)_2$ molecule, as shown in Figure 4, this molecule was predicted to have a $^1A_1$ ground state with planar geometry.

Assignment. *ScO*. The 954.7 cm^{-1} band is assigned to the ScO molecule based on previous work. Present DFT calculations predicted a $^2\Sigma^+$ ground state with the Sc−O stretching vibration at 999.5 cm^{-1}, which is in good agreement with previous work.[7,29]

HScOH. The 1482.6 cm^{-1} absorption increased on annealing and was totally eliminated on full arc mercury lamp photolysis. It shifted to 1068.5 cm^{-1} with D_2O and gave an isotopic H/D ratio of 1.3876. A band at 713.0 cm^{-1} exhibited the same annealing and photolysis behavior with the 1482.6 cm^{-1} band, it shifted to 689.1 cm^{-1} with D_2O and to 693.6 cm^{-1} with $H_2{}^{18}O$ reagent. These two bands are assigned to the Sc−H and Sc−OH stretching vibrations of the HScOH molecule, in agreement with the Hauge group.[7] Present DFT calculations predicted that the HScOH molecule has a $^2A'$ ground state with the Sc−H and Sc−OH stretching vibrations at 1529.5 and 717.1 cm^{-1}, just 46.9 and 4.1 cm^{-1} higher than the observed values, which provides excellent support for the assignment.

HScO. The 1391.1 and 922.3 cm^{-1} bands were not reported on thermal Sc atom reactions.[7] These two bands tracked through all the experiments, suggesting different vibrational modes of the same molecule. These two bands were observed after sample

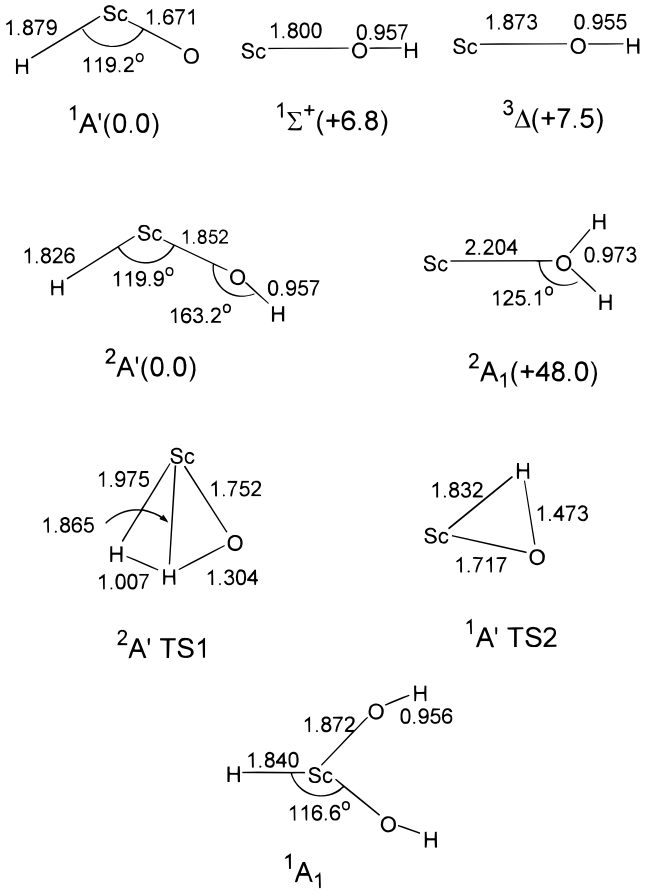

Figure 4. Calculated geometric parameters for the Sc + H_2O reaction products and transition states (bond length in Å, bond angle in degree, relative energies for different isomers are given in parentheses in kcal/mol).

TABLE 3: Calculated Vibrational Frequencies (cm^{-1}) and Intensities (km/mol) for ScOH, HScO, and the Transition State (TS2) on the ScOH → HScO Reaction Path

molecule	frequency (intensity)
$ScOH(^1\Sigma^+)$	3958.8 (349), 778.8 (120), 322.5 (204)
ScOD	2886.7 (233), 761.6 (112), 244.3 (114)
$Sc^{18}OH$	3945.4 (337), 748.5 (111), 320.0 (202)
$ScOH(^3\Delta)$	3976.3 (178), 691.3 (100), 303.9 (212)
$HScO(^1A')$	1459.2 (317), 977.4 (302), 391.0 (203)
DScO	1046.1 (121), 975.7 (335), 294.0 (103)
$HSc^{18}O$	1459.0 (320), 936.8 (281), 389.3 (202)
TS2	1536.7 (86), 932.9 (182), 1342.0i (1910)

TABLE 4: Calculated Vibrational Frequencies (cm^{-1}) and IR Intensities (km/mol) for the HScOH, $ScOH_2$, and the Transition State (TS1) on the HScOH → H_2 + ScO Reaction Path

$HScOH(^2A')$	DScOD	$HSc^{18}OH$	$ScOH_2(^2A_1)$	TS1
3956.1 (230)	2883.3 (167)	3942.8 (219)	3710.8 (4)	1885.3 (99)
1529.5 (516)	1093.8 (269)	1529.4 (516)	3602.0 (533)	1670.8 (194)
717.1 (212)	700.0 (189)	690.0 (201)	555.0 (189)	1224.2 (21)
368.6 (162)	279.0 (95)	365.8 (160)	322.3 (17)	911.6 (205)
347.1 (160)	265.3 (89)	344.7 (156)	322.0 (10)	892.3 (132)
325.3 (82)	236.1 (45)	324.1 (83)	150.1i (59)	1347.3i (743)

deposition and increased on broadband photolysis. The 1391.1 cm^{-1} band exhibited a very small shift when the isotopic $H_2{}^{18}O$ sample was used but was shifted to 1004.2 cm^{-1} with D_2O, the isotopic H/D ratio 1.3853 indicating that it is due to a Sc−H stretching vibration. In concert, the 922.3 cm^{-1} band showed no isotopic shift with the D_2O sample but was shifted to 884.3 when the $H_2{}^{18}O$ sample was used. The isotopic 16/18 ratio

1.0430 is very close to the diatomic ScO ratio (1.0434) observed in solid argon, suggesting that this band is due to a terminal Sc−O stretching vibration. Accordingly, these two bands are assigned to the Sc−H and Sc−O stretching vibrations of the HScO molecule. The assignment is further supported by DFT calculations. Present calculations predicted that the HScO molecule has a $^1A'$ ground state with a HScO angle of 119.2°. The Sc−H and Sc−O stretching vibrations were predicted at 1459.2 and 977.4 cm^{-1}, which must be scaled by 0.953 and 0.977 to match the experimental values. The higher energy mode was calculated to shift by 413.1 and 0.2 cm^{-1} with D_2O and $H_2{}^{18}O$, respectively, while the lower mode was calculated to shift by 1.7 and 40.6 cm^{-1} with D_2O and $H_2{}^{18}O$, which are in good agreement with the observed argon matrix values.

ScOH. A weak band at 765.6 cm^{-1} was produced on sample deposition, it decreased on annealing and was destroyed on broadband photolysis. This band was not observed in previous thermal Sc atom experiments; it underwent oxygen-18 and deuterium shifts of 28.7 and 15.1 cm^{-1}, respectively. Mixed isotopic sample experiments indicted that only one H and one O atom are involved in this vibrational mode. This band is assigned to the Sc−OH stretching vibration of the ScOH molecule. DFT calculation predicted that the ScOH molecule has a $^1\Sigma^+$ ground state with a Sc−OH stretching vibration at 778.8 cm^{-1}. The calculated isotopic frequency ratios ($^{16}O/^{18}O$: 1.0405, H/D:1.0226) are in good agreement with observed values ($^{16}O/^{18}O$:1.0389, H/D:1.0201). Previous thermal Sc + D_2O study assigned a 699.2 cm^{-1} band to the ScOD molecule,[7] we believe that this identification is in error.

$HSc(OH)_2$. The 729.6 cm^{-1} band was also observed in previous thermal atom experiments.[7] This band appeared on annealing. Isotopic substitution experiments indicated that this is a Sc−OH stretching vibration and two OH units are involved. This band was tentatively assigned to the $HSc(OH)_2$ molecule previously. A weak band at 1418.3 cm^{-1} tracked with the 729.6 cm^{-1} band and is due to a Sc−H stretching vibration. Our DFT calculations on $HSc(OH)_2$ find a $^1A_1$ ground state with planar geometry (see Figure 4). The antisymmetric HO−Sc−OH, symmetric HO−Sc−OH, and Sc−H stretching vibrations were calculated at 756.7, 683.6, and 1546.4 cm^{-1} with 431:96:468 relative intensities. The symmetric HO−Sc−OH stretching vibration was not observed due to weakness.

There is no evidence for scandium hydride molecules. Scandium monohydride has been the subject of several gas-phase spectroscopic and theoretical studies.[27,28] The ground state of ScH in the gas phase has been determined to be $^1\Sigma^+$ with a $^3\Delta$ state lying slightly higher in energy. Our DFT calculations predicted a vibrational fundamental of 1483.8 cm^{-1} for the $^3\Delta$ state and 1626.3 cm^{-1} for the $^1\Sigma^+$ state.

Reaction Mechanism. Co-condensation of laser-ablated Sc atoms and water molecules in excess argon resulted in the insertion reaction (1) to form HScOH as the major product. Our

$$Sc(^2D) + H_2O(^1A_1) \rightarrow HScOH(^2A') \quad (1)$$

DFT calculation showed that this reaction is exothermic by about 61.5 kcal/mol. Weak ScO, ScOH, and HScO molecules were also observed on sample deposition, indicating that some HScOH molecules were decomposed in the laser ablated plume before deposition at the low temperature.

The HScOH absorptions increased on matrix sample annealing, suggesting that the insertion reaction require no activation energy. On broadband photolysis, the HScOH absorptions were destroyed, while the ScO absorption greatly increased. To have a better understanding of this reaction, potential energy surfaces

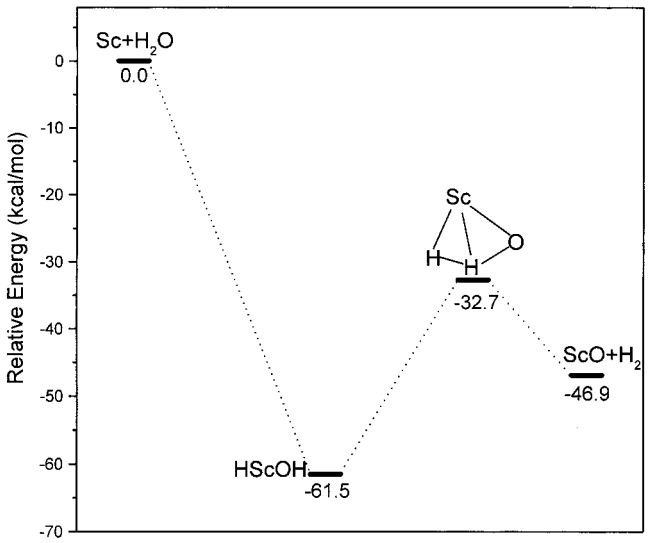

Figure 5. Potential energy surface for the Sc + H_2O reaction at the B3LYP/6-311++G(d,p) level. Energies given are in kcal/mol and are relative to the separated ground-state reactants: $Sc(^2D)$ + $H_2O(^1A_1)$.

starting from Sc + H_2O were calculated at the B3LYP/6-311++G(d,p) level, as shown in Figure 5. Recent studies on Sc^+ + H_2O reactions have shown that the first step of this reaction is the formation of a Sc^+OH_2 ion−molecule complex; then through a transition state, one hydrogen atom is passed from oxygen to the metal, leading to the insertion $HScOH^+$ molecule.[13] For Sc atom reactions, our DFT calculations predicted that the $ScOH_2$ complex is a first-order saddle point, and no evidence was presented for the $ScOH_2$ complex in our experiments. The ground-state Sc atom reactions with H_2O molecules to form the inserted HScOH molecules proceed spontaneously without energy barrier. The HScOH molecule undergoes H_2 elimination through a transition state (TS1). This transition state has a four-centered structure; it is about 28.8kcal/mol higher in energy than the HScOH molecule. As can be seen in Figure 4, the H−H distance is 1.007 Å; the two Sc−H distances 1.975 and 1.865 Å and the Sc−O distance 1.752 Å are significantly longer than that in the HScOH molecule. The one imaginary frequency corresponds to the H−H bond formation and the O−H bond breaking.

The HScO absorptions were markedly enhanced on photolysis; there are two major possible reactions to form this molecule,

$$HScOH(^2A') \rightarrow HScO(^1A') + H \quad (2)$$

$$ScOH(^1\Sigma^+) \rightarrow HScO(^1A') \quad (3)$$

Reaction 2 is predicted to be endothermic, while reaction 3 is slightly exothermic. If reaction 2 takes place in the matrix, the hydrogen atom will back-react to form the HScOH molecule due to the matrix cage effect. As can be seen in Figure 1, visible range photolysis eliminated the ScOH absorption with no obvious effect on the HScOH absorptions, while the HScO absorptions greatly increased. In previous thermal Sc atom experiments,[7] the HScO molecule was not formed on photolysis, as no ScOH was present. All this evidence suggests that reaction 3 is the dominant process for the formation of HScO under photolysis. Figure 6 shows the doublet potential energy surface of the ScOH → HScO reaction. The transition state (TS2) lies above the ScOH molecule by about 28.9 kcal/mol at the B3LYP/6-311++G(d,p) level of theory. This transition state has Sc−H, Sc−O, and O−H bond lengths of 1.832, 1.717, and 1.473

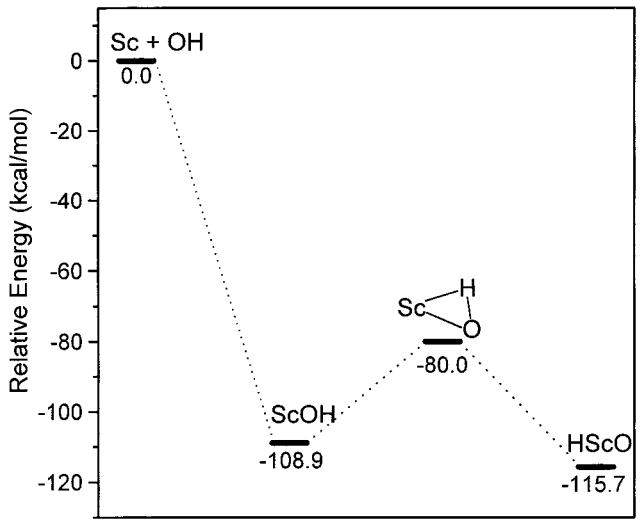

Figure 6. Potential energy surface for the Sc + OH reaction at the B3LYP/6-311++G(d,p) level. Energies given are in kcal/mol and are relative to the separated ground-state reactants: $Sc(^2D) + OH(^2\Pi)$.

Å, respectively. The one imaginary frequency confirms that it is a real transition state.

The $HSc(OH)_2$ molecule appeared on annealing; this molecule may form by reactions of the HScOH molecule with the OH radical or the ScOH molecule with H_2O.

Conclusions

The reactions of Sc atoms with water molecules have been reinvestigated using the laser-ablation technique and density functional theoretical calculations. In agreement with previous thermal atom work, the HScOH molecules are formed by direct insertion reaction that requires no activation energy. New absorption at 765.6 cm^{-1} is also observed and is assigned to the ScOH molecule. The ScOH molecule undergoes photoinduced rearrangement to the HScO molecule, which is characterized by Sc−H and Sc−O stretching vibrations at 1391.1 and 922.3 cm^{-1}. UV−visible photolysis of the HScOH causes H_2 elimination from a four-centered transition state and produces the metal monoxide ScO. The aforementioned species have been identified by isotopic substitution experiments as well as density functional theoretical calculations. Potential energy surfaces for the above-mentioned reactions have also been calculated, and important transition states on the reaction paths have been obtained.

Acknowledgment. We acknowledge contributions from Prof. Q. Z. Qin. This work is supported by the Chinese NKBRSF.

References and Notes

(1) Clemmer, D. E.; Aristov, N.; Armentrout, P. B. *J. Phys. Chem.* **1993**, *97*, 544.
(2) Chen, Y. M.; Clemmer, D. E.; Armentrout, P. B. *J. Phys. Chem.* **1994**, *98*, 11490.
(3) Clemmer, D. E.; Chen, Y. M.; Aristov, N.; Armentrout, P. B. *J. Phys. Chem.* **1994**, *98*, 7531.
(4) Agreiter, J. K.; Knight, A. M.; Duncan, M. A. *Chem. Phys. Lett.* **1999**, *313*, 162.
(5) Liu, K.; Parson, J. M. *J. Chem. Phys.* **1978**, *68*, 1794.
(6) Kauffman, J. W.; Hauge, R. H.; Margrave, J. L. *J. Phys. Chem.* **1985**, *89*, 3541.
(7) Kauffman, J. W.; Hauge, R. H.; Margrave, J. L. *J. Phys. Chem.* **1985**, *89*, 3547.
(8) Hauge, R. H.; Kauffman, J. W.; Margrave, J. L. *J. Am. Chem. Soc.* **1980**, *102*, 6005.
(9) Knight, L. B. Jr.; Gregory, B.; Cleveland, J.; Arrington, C. A. *Chem. Phys. Lett.* **1993**, *204*, 168.
(10) Tilson, J. L.; Harrison, J. F. *J. Phys. Chem.* **1991**, *95*, 5097.
(11) Ye, S. *THEOCHEM* **1997**, *417*, 157.
(12) Irigoras, A.; Fowler, J. E.; Ugalde, J. M. *J. Phys. Chem. A* **1998**, *102*, 293.
(13) Irigoras, A.; Fowler, J. E.; Ugalde, J. M. *J. Am. Chem. Soc.* **1999**, *121*, 574.
(14) Irigoras, A.; Fowler, J. E.; Ugalde, J. M. *J. Am. Chem. Soc.* **1999**, *121*, 8549.
(15) Chertihin, G. V.; Andrews, L. *J. Chem. Phys.* **1998**, *108*, 6404.
(16) Chertihin, G. V.; Saffel, W.; Yustein, J. T.; Andrews, L.; Neurock, M.; Ricca, A.; Bauschlicher, C. W., Jr. *J. Phys. Chem.* **1996**, *100*, 5261.
(17) Zhou, M. F.; Liang, B. Y.; Andrews, L. *J. Phys. Chem. A* **1999**, *103*, 2013.
(18) Chen, M. H.; Wang, X. F.; Zhang, L. N.; Yu, M., Qin, Q. Z. *Chem. Phys.* **1999**, *242*, 81.
(19) Burkholder, T. R.; Andrews, L. *J. Chem. Phys.* **1991**, *95*, 8697.
(20) Frisch, M. J.; Trucks, G. W.; Schlegel, H. B.; Scuseria, G. E.; Robb, M. A.; Cheeseman, J. R.; Zakrzewski, V. G.; Montgomery, J. A., Jr.; Stratmann, R. E.; Burant, J. C.; Dapprich, S.; Millam, J. M.; Daniels, A. D.; Kudin, K. N.; Strain, M. C.; Farkas, O.; Tomasi, J.; Barone, V.; Cossi, M.; Cammi, R.; Mennucci, B.; Pomelli, C.; Adamo, C.; Clifford, S.; Ochterski, J.; Petersson, G. A.; Ayala, P. Y.; Cui, Q.; Morokuma, K.; Malick, D. K.; Rabuck, A. D.; Raghavachari, K.; Foresman, J. B.; Cioslowski, J.; Ortiz, J. V.; Baboul, A. G.; Stefanov, B. B.; Liu, G.; Liashenko, A.; Piskorz, P.; Komaromi, I.; Gomperts, R.; Martin, R. L.; Fox, D. J.; Keith, T.; Al-Laham, M. A.; Peng, C. Y.; Nanayakkara, A.; Gonzalez, C.; Challacombe, M.; Gill, P. M. W.; Johnson, B.; Chen, W.; Wong, M. W.; Andres, J. L.; Gonzalez, C.; Head-Gordon, M.; Replogle, E. S.; Pople, J. A. *Gaussian 98*, Revision A.7; Gaussian, Inc.: Pittsburgh, PA, 1998.
(21) Becke, A. D. *J. Chem. Phys.* **1993**, *98*, 5648.
(22) Lee, C., Yang, E., Parr, R. G. *Phys. Rev. B* **1988**, *37*, 785.
(23) Bauschlicher, C. W., Jr.; Ricca, A.; Partridge, H.; Langhoff, S. R. In *Recent Advances in Density Functional Theory*; Chong, D. P., Ed.; World Scientific Publishing: Singapore, 1997; Part II.
(24) Bytheway, I., Wong, M. W. *Chem. Phys. Lett.* **1998**, *282*, 219.
(25) McLean, A. D.; Chandler, G. S. *J. Chem. Phys.* **1980**, *72*, 5639. Krishnan, R., Binkley, J. S.; Seeger, R., Pople, J. A. *J. Chem. Phys.* **1980**, *72*, 650.
(26) Wachter, J. H. *J. Chem. Phys.* **1970**, *52*, 1033. Hay, P. J. *J. Chem. Phys.* **1977**, *66*, 4377.
(27) Chong, D. P.; Langhoff, S. R.; Bauschlicher, C. W., Jr.; Walch, S. P.; Partridge, H. *J. Chem. Phys.* **1986**, *85*, 2850 and references therein.
(28) Ram, R. S.; Bernath, P. F. *J. Chem. Phys.* **1996**, *105*, 2668 and references therein.
(29) Chertihin, G. V.; Andrews, L.; Rosi, M.; Bauschlicher, C. W., Jr. *J. Phys. Chem. A* **1997**, *101*, 9085.